Pediatrics International (2005) **47**, 616–621

Original Article

Different patterns of cytokines, ECP and immunoglobulin profiles at two adverse drug reactions in a patient

YUKOH AIHARA,[1] SHUICHI ITO,[1] MICHIKO AIHARA,[2] YOSHINORI KOBAYASHI[3] AND SHUMPEI YOKOTA[3]

Departments of [1]Pediatrics and [2]Dermatology, Yokohama City University Medical Center, [3]Department of Pediatrics, Yokohama City University School of Medicine, Yokohama, Japan

Abstract

Objectives: Drug-induced hypersensitivity syndrome (HS) is a rare but life-threatening disease. We experienced carbamazepine-induced HS in a 14-year-old boy, who had cefaclor-induced cutaneous eruptions 15 months later. To clarify the mechanisms of HS and the differences between two diseases we studied this case in detail.

Methods: We investigated the associated viral agents by polymerase chain reaction and the specific antibodies. We also studied the mechanism of diseases by measuring chemical mediators including cytokines, ECP and immunoglobulins.

Results: The patient was diagnosed as having carbamazepine-induced HS associated with reactivation of human herpesvirus 6 based on the clinical course and laboratory data including drug-induced lymphocyte stimulation tests. Similarly, the diagnosis of cefaclor-induced eruption without any viral reactivation was made. Serum levels of IFN-γ, IL-6, TNF-α, IL-5 and ECP were increased significantly at HS but mildly at cefaclor-induced eruptions. Furthermore, we detected transient hypogammaglobulinemia only at HS.

Conclusions: This is the first report of anticonvulsant-induced HS followed by antibiotic-induced eruptions in a patient. In addition, we demonstrated difference in serum levels of inflammatory cytokines, immunoglobulins, activated eosinophils and viral reactivation between these diseases. This case would contribute to the understanding of the pathophysiology of adverse drug reactions including HS.

Key words adverse reaction, cytokines, drug, hypersensitivity syndrome, immunoglobulin, pathophysiology, viral reactivation.

Anticonvulsant-induced hypersensitivity syndrome (HS) is an acute and life-threatening disease, which is characterized by severe multiorgan hypersensitivity reactions.[1–6] However, the pathophysiology of HS remains unknown.[3,6] Recently, some virus infections, particularly human herpesvirus family, were reported as being major precipitating factors of the disease.[7–11] In contrast, drug-induced cutaneous eruption is also an acute and self-limited but seldom life-threatening disease. We reported a pediatric case of HS due to carbamazepine (CBZ) and associated with reactivation of human herpesvirus 6 (HHV6) infection and transient hypogammaglobulinemia.[7] Surprisingly, he had cefaclor-induced cutaneous eruptions with generalized symptoms 15 months later. Thus, we report here this rare case and demonstrate the differences in mechanisms between these two diseases.

Correspondence: Yukoh Aihara, Department of Pediatrics, Yokohama City University Medical Center, 4-57 Urafune-cho, Minami-ku, Yokohama 232-0024, Japan.
Email: yaihara1@urahp.yokohama-cu.ac.jp

Received 17 June 2004; revised 28 December 2004; accepted 28 February 2005.

Case

Episode 1

The patient, a 14-year-old boy, had been diagnosed as having epilepsy and had been treated with valproate sodium (VPA, 600 mg daily) since 20 April 2001. However, convulsions recurred, and CBZ (200 mg daily) was added on 6 July 2001 (episode 1, day 1). On 23 July, he developed a fever followed by skin eruptions on 25 July. He was then treated with cefaclor (CCL) (600 mg daily) as a bacterial infection was suspected. However, generalized erythema and fever persisted along with slightly elevated serum levels of liver enzymes on 26 July. He was therefore admitted to the nearby hospital on the same day. Drug-induced eruptions were suspected, and CBZ and CCL were discontinued immediately. However, his

condition and laboratory data exhibited further deterioration. Thus, he was transferred to our hospital on 3 August (day 29). Apart from epilepsy and mild mental retardation, there were no abnormalities in his previous history and his family history was unremarkable.

On admission, he had facial and body angiedema, generalized lymphadenopathy, mild hepatosplenomegaly, and generalized erythema without erosions. His body temperature was 38.5°C. The results of laboratory tests were as follows: white blood cell count 31 700/μL (eosinophils 11%, atypical lymphocyte 12.5%), red blood cells count 446×10^4/μL, hemoglobin 13.6 g/dL, platelets count 16.9×10^4/dL, CRP 1.8 mg/dL, total protein 5.2 g/dL, albumin 3.1 g/dL, AST 137 IU/L (normal 14–32), ALT 202 IU/L (normal 9–25), LDH 714 IU/L (normal 116–199), BUN 10 mg/dL, and creatinine 0.69 mg/dL. Blood coagulation studies demonstrated a fibrin/fibrinogen degradation product (FDP-E) level of 314 ng/mL (normal <60). Immunological analyses were negative for antinuclear antibody, and the serum level of immune complex was 12.8 mg/L (anti-C3d method, normal <13.0). Serum levels of CH50, C3 and C4 were 35 U/mL, 109 mg/dL and 24 mg/dL, respectively. Soluble IL-2R was 13 100 U/mL (normal 220–530), 2–5 oligoadenylic acid synthetase (2–5 AS) 213 pmol/dL (normal <100), β2-microglobulin 5.07 mg/L (normal 0.85–1.71). Urinalysis was positive for protein 1+ and occult blood 1+.

The patient was diagnosed as having CBZ-induced HS. Therefore, intravenous methylprednisolone (mPSL, 30 mg/kg/day) pulse therapy was started, followed by oral prednisolone (PSL, 30 mg daily). On this treatment, his clinical symptoms and abnormal laboratory findings gradually improved. After stopping mPSL pulse therapy, there was mild relapse of disease activity. This was controlled with betamethasone (8 mg daily). Then the dose of oral steroid was gradually tapered with complete withdrawal after 5 weeks. For 1 year and 3 months after the end of therapy, no abnormal clinical episodes were induced with VPA and clonazepam (CZP).

Episode 2

The patient had folliculitis on the face since the beginning of September 2002 and was treated with CCL (600 mg daily) at the nearby hospital on 20 September 2002 (episode 2, day 1). On 22 September, he developed a fever of more than 39°C with skin eruptions on the legs. On 23 September, CCL was stopped and changed to midecamycin (MDM). However, his condition including skin eruptions deteriorated, and he was transferred to our hospital again on 25 September 2002 (episode 2, cay 6) because of suspected drug-induced HS.

On admission, he had generalized maculopapular eruptions without erosions. However, there was neither lymphadenopathy, hepatosplenomegaly nor angiedema. His body temperature was 38.3°C. The results of laboratory tests were as follows: white blood cells count 7200/μL (eosinophils 9%, atypical lymphocyte 1.5%), red blood cells count 494×10^4/μL, hemoglobin 14.9 mg/dL, platelets count 14.0×10^4/μL, CRP 1.2 mg/dL, total protein 7.9 g/dL, albumin 4.8 mg/dL, AST 13 IU/L, ALT 11 IU/L, LDH 191 IU/L, BUN 16 mg/dL, and creatinine 0.67 mg/dL. Blood coagulation studies demonstrated FDP-E level of 80 ng/mL. Immunological analyses were negative for antinuclear antibody, and the serum level of immune complex was 10.9 μg/mL. Serum levels of CH50, C3 and C4 were 48.1 U/mL, 133 mg/dL and 29 mg/dL, respectively. Soluble IL-2R was 4120 U/mL, 2–5 AS 132 pmol/dL, and β2-microglobulin 2.12 mg/L. Urinalysis was unremarkable.

This time his condition including skin rashes and laboratory data were not as severe. We suspected drug eruption due to CCL. Betamethasone (8 mg daily) was started on the admission day. His condition improved significantly earlier than the first episode. There was no relapse of disease activity with tapering of steroid, and oral steroid was withdrawn completely on 15 October 2002. At present, 11 months after stopping the steroid therapy, there has been no adverse drug reaction.

Further studies were performed to clarify the mechanisms and causative factors of the two episodes. Virological investigation was performed. At the first episode, serum levels of IgG but not IgM antibody against HHV6 increased from 1:10 dilution to 1:10 240 (Table 1). There were no significant changes of antibodies against HHV7, CMV, EBV, HSV, VZV and Parvovirus B19. Analysis of viral genomes using real-time PCR[12] demonstrated increased HHV6 but not HHV7 viral DNA in 10^6 peripheral blood cells (3.5×10^5 copies) on day 32 (Table 1). In addition, CMV DNA was not detected in his sera. At the second episode, there were no significant changes of specific antibody against HHV6, HHV7 (Table 1) or other viruses listed above. However, real-time PCR data demonstrated slight increase of HHV7 viral DNA (4.1×10^3) but not HHV6 DNA at day 33.

Serum levels of immunoglobulins are shown in Table 2. The serum levels of IgG at the first episode increased from 649 mg/dL on day 29 to 1169 mg/dL on day 55. Similarly, IgA and IgM increased. These data demonstrate transient hypogammaglobulinemia. We also studied the serum levels of IgG subclasses[13] (Table 2). In accordance with the changes in total IgG, those in IgG1, IgG2, IgG3, and IgG4 increased. In particular, IgG4 and IgM increased significantly. However, there were no increases in serum levels of immunoglobulin classes or subclasses at the second episode. Those levels were instead decreased (Table 2).

A drug-induced lymphocyte stimulation test (DLST) using peripheral blood mononuclear cells was performed for CBZ and CCL on 3 August 2001 (episode 1, day 29). The results of the stimulation index to the control were positive against

Table 1 Profiles of the specific antibodies and DNA of human herpes viruses at two episodes in the patient

Virus	Ig class /genome	Episode 1				Episode 2		
		Day 29	Day 32	Day 39	Day 75	Day 6	Day 19	Day 33
HHV6	IgM[1]	<10	ND	<10	ND	<10	<10	ND
	IgG[1]	10	ND	5120	10 240[†]	320	160	ND
	DNA[2]	ND	3.5×10^5	1.9×10^4	6.3×10^3	8.4×10^1	ND	7.3×10^1
HHV7	IgM[1]	<10	ND	<10	ND	<10	ND	<10
	IgG[1]	80	ND	160	ND	80	ND	20
	DNA[2]	ND	2.2×10^3	ND	1.4×10^3	2.5×10^2	1.2×10^3	4.1×10^3
CMV	IgM[3]	0.38	0.25	0.31	ND	<0.8	<0.8	ND
	IgG[3]	<2.0	<2.0	<2.0	ND	<2.0	<2.0	ND
	DNA[2]	ND	$<2.0 \times 10^1$	ND	$<2.0 \times 10^1$	ND	ND	ND
EBV VCA	IgM[1]	<10	<10	<10	ND	<10	<10	ND
	IgG[1]	<10	<10	<10	ND	<10	<10	ND

[†]Determined at day 52. Day 1 represents the first day of his treatment with CBZ or with CCL at each episode. On day 29 at the first episode and on day 6 at the second one he admitted to our hospital. This table was modified from reference 7.[7]

FA, fluorescent antibody method (1:x dilution); 2, PCR; real-time PCR (copies/10^6 cells); 3, EIA; enzyme immunoassay (unit/mL); ND, not determined; Ig, immunoglobulin.

Table 2 Changes of serum levels of immunoglobulin classes and IgG subclasses at two episodes in the patient

Immunoglobulin	Episode 1			Episode 2		
	Day 29	Day 55	% Increase	Day 6	Day 33	% Increase
IgG	649	1169	180	1160	990	−15
IgG1	384	773	201	640	510	−20
IgG2	247	365	148	490	453	−7
IgG3	13	25	192	22	19	−14
IgG4	0.4	3.5	875	8.4	7.9	−6
IgA	80	118	148	124	102	−12
IgM	47	204	434	76	79	101
IgE	550	ND	ND	783	931	119

See Table 1 footnotes. This table was modified from reference 7.[7] Unit of all immunoglobulins was mg/dL except IgE (IU/mL).
ND; not determined.

CBZ (726%) and negative against CCL (77%) (Table 3). This suggested that the patient had been sensitized with CBZ but not CCL at the first episode. In addition, DLST for CCL and MDM were carried out on 25 September 2002 (episode 2, day 6). The results were positive against CCL (1746%) and negative against MDM (113%) (Table 3). This suggested that the causative agent of the second episode was CCL. Furthermore, on 15 August 2003, DLST against CBZ and CCL were done. The results were positive against both drugs, such as CBZ (313%) and CCL (1572%) (Table 3).

We measured serum levels of seven cytokines using Cytometric Bead Array (BD PharMingen, San Diego, CA, USA)[14] and Human IL-6 ELISA Ready-SET (eBioscience, San Diego, CA, USA) and ECP by Uni-CAP ECP (Pharmacia Biotech, Piscataway, NJ, USA). At the first episode, serum levels of IL-5, IFN-γ and ECP were increased on day 29 and decreased dramatically on day 39. Similarly, IL-6 was increased. However, IL-4 was not detected at any time point (Fig. 1). In contrast, at the second episode on day 6, there were slight increases in IL-5, IFN-γ, IL10, IL-6 and ECP in his sera. However, TNF-α was not detected at any point (Fig. 1).

Discussion

At the first episode we diagnosed drug-induced HS caused by CBZ based on positive DLST, periods of exposure to the drug and typical clinical manifestations.[7] In this patient, typical clinical features developed 17 days after the start of CBZ. Regardless of discontinuation of the causative drug, his condition did not change and he exhibited blood coagulation abnormalities and nephritis. His symptoms persisted for 10 days before the start of mPSL pulse therapy. In contrast, at the second episode, we diagnosed CCL-induced rashes based on positive DLST, exposure to the drug and the milder

Table 3 Changes of the results of DLST at two episodes in the patient

Drugs	Episode 1 Day 29, 3 August 2001	Episode 2 Day 6, 25 September 2002	Afterwards 15 August 2003
CBZ	726%	ND	313%
CCL	77%	1746%	1572%
MDM	ND	113%	ND

See Table 1 footnotes. The results of stimulation index were shown as percentages against the control values.

CBZ, carbamazepine; CCL, cefaclor; MDM, midecamycin; ND, not determined.

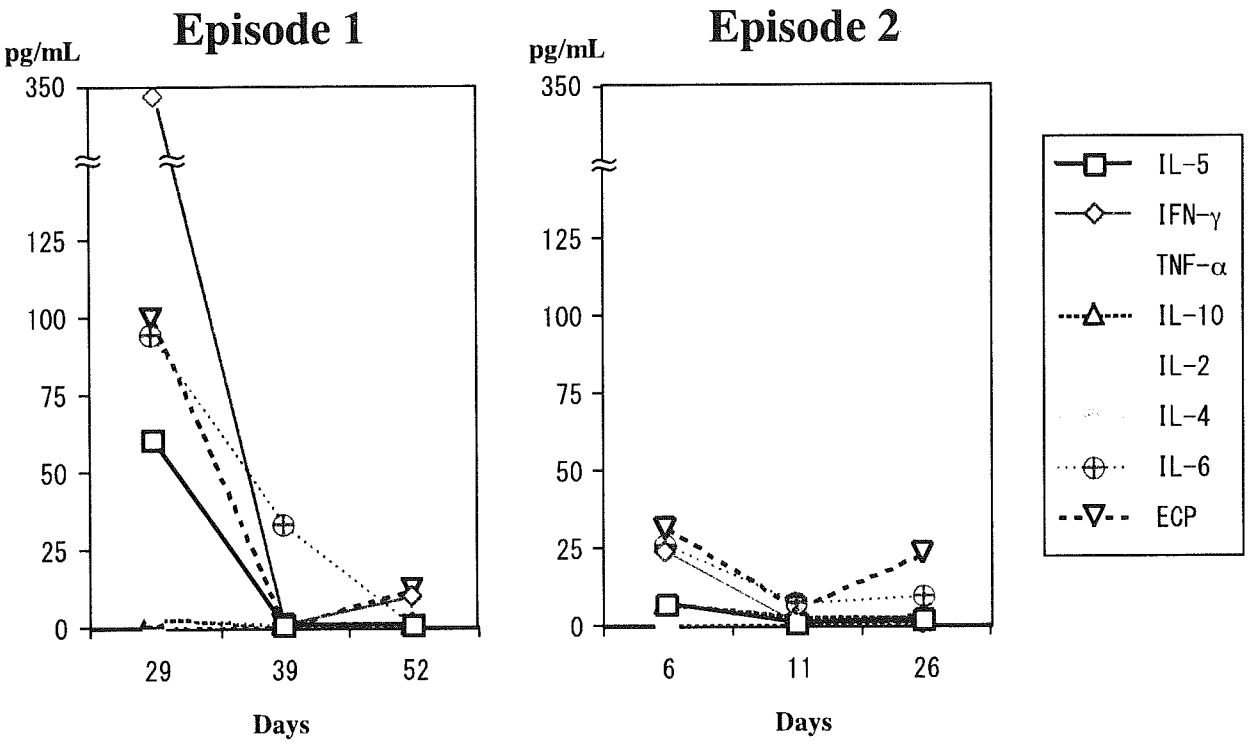

Fig. 1 Serum levels of cytokines and ECP at two episodes. Normal ranges of all seven cytokines in serum are <0.1 pg/mL and that of ECP in serum is <5.0 pg/mL.

clinical manifestations which developed 3 days after the start of CCL administration. This was at least the second time the patient had taken CCL. At the first episode, the result of DSLT to CCL was negative, suggesting that during the 15 months between two episodes sensitization to CCL was established.

The pathophysiology of HS, in particular, the association of reactivation of a certain virus and drug-induced hypersensitivity reactions, has also not been elucidated. In most of the recently reported cases, the associated viruses were shown to be members of the human herpesvirus family, particularly HHV6.[7-11] The association of HHV6 but not HHV7 reactivation in our patient at the first episode was determined by the significantly increased levels of specific IgG antibodies and HHV6 DNA copies in peripheral blood cells by real-time PCR. However, we could not detect an association of reactivation of HHV infection except for a slight increase in HHV7 genomes at the second episode. This difference might explain in part the severity of clinical manifestations and the difference in numbers of atypical lymphocytes in peripheral blood between these two episodes. Moreover, we could at least rule out the possibility of other associated viral infections including CMV, EBV, HSV, VZV and Parvovirus B19 based on the results for specific antibodies and/or viral genome in his peripheral blood at both episodes. In addition, the difference in time courses of these episodes might account for the difference in reactivation of HHV infection.

Drug-induced HS and drug eruptions are believed to be immune-mediated diseases. Many factors, including positive patch tests and DLST, suggest an immune-mediated mechanism for these diseases.[2,7,15] However, there are few reports available dealing with cytokine profiles in sera but not in local skin lesions in patients with this HS or with drug-induced cutaneous eruptions.[16,17] We demonstrated significant increases in IL-5, IL-6 and IFN-γ but not IL-4 at HS in the patient's serum before steroid therapy. However, the magnitude of increase in levels of inflammatory cytokines was lower at CCL-induced skin rashes. Furthermore, it was shown that eosinophilia was more prominent at HS than at drug-induced rashes, in parallel with the increase of IL-5 and ECP in his sera. Based on these data, we suspect that not only inflammatory cytokines but also activated eosinophils play important roles in HS. This is supported by a report of significant roles of activated eosinophils induced by IL-5 in drug-induced cutaneous eruptions.[16]

Concerning the possibility of immunemodulation in patients with HS but not drug-induced rashes, the association of reactivation of HHV6 should be considered. Since it is known that cells infected with HHV6, in vitro, produce several cytokines including IL-6, IFN-α and TNF-α.[18] However, immunosuppressive effects of HHV6 on T cell function in vitro have also been reported.[19] In addition, it is known that treatment with anticonvulsants sometimes induces hypogammaglobulinemia in patients with epilepsy.[7,10,20,21] However, the mechanism of this is not well understood. In our patient, we detected transient hypogammaglobulinemia at the first but not the second episode. This may explain in part the association of immunosuppression and reactivation of HHV6 in our patient at the first episode. However, this alone would not explain the pathophysiology of HS.

Cross-reactivity among anticonvulsants is known in patients with HS.[5] However, our patient experienced two relatively severe adverse drug reactions with different kinds of drugs such as anticonvulsant and antibiotic. Although the frequency of skin rashes in children treated with cefaclor was the highest (4.79%) among oral antibiotics,[22] we suspect that there is a predisposition in our patient for adverse drug reactions.[5] In addition, based on the results of DLST we demonstrated that the memory cells to CBZ and CCL still exist significantly in his peripheral blood even under the strict elimination of those drugs after 1 and/or 2 years from the episodes.

We demonstrated that the magnitudes of inflammation in two different kinds of adverse drug reactions paralleled the clinical manifestations and serum levels of chemical mediators in our patient. In addition, it was shown in our patient that there were more associated factors in HS such as the reactivation of HHV infection and hypogammaglobulinemia. We believe that our case contributes to an understanding of the pathophysiology of HS, and that further investigations should be undertaken to clarify this.

References

1 Chopra S, Levell NJ, Cowley G, Gilkes JJ. Systemic corticosteroids in the phenytoin hypersensitivity syndrome. *Br. J. Dermatol.* 1996; **134**: 1109–12.

2 Scerri L, Shall L, Zaki I. Carbamazepine-induced anticonvulsant hypersensitivity syndrome – pathogenic and diagnostic considerations. *Clin. Exp. Dermatol.* 1993; **18**: 540–2.

3 Sullivan JR, Shear NH. The drug hypersensitivity syndrome: what is the pathogenesis? *Arch. Dermatol.* 2001; **137**: 357–64.

4 Shear NH, Spielberg SP. Anticonvulsant hypersensitivity syndrome. *J. Clin. Invest.* 1988; **82**: 1826–32.

5 Kleier RS, Breneman DL, Boiko S. Generalized pustulation as a manifestation of the anticonvulsant hypersensitivity syndrome. *Arch. Dermatol.* 1991; **127**: 1361–4.

6 Gruchalla RS. Drug metabolism, danger signals, and drug-induced hypersensitivity. *J. Allergy Clin. Immunol.* 2001; **108**: 475–88.

7 Aihara Y, Ito S, Kobayashi Y, Yamakawa Y, Aihara M, Yokota S. Carbamazepine-induced hypersensitivity syndrome associated with transient hypogammaglobulinemia and reactivation of human herpesvirus 6 infection demonstrated by real-time quantitative PCR. *Br. J. Dermatol.* 2003; **149**: 165–9.

8 Suzuki Y, Inagi R, Aono T, Yamanishi K, Shiohara T. Human herpesvirus 6 infection as a risk factor for the development of severe drug-induced hypersensitivity syndrome. *Arch. Dermatol.* 1998; **134**: 1108–12.

9 Tohyama M, Yahata Y, Yasukawa M *et al.* Severe hypersensitivity syndrome due to sulfasalazine associated with reactivation of human herpesvirus 6. *Arch. Dermatol.* 1998; **134**: 1113–17.

10 Descamps V, Valance A, Edlinger C *et al.* Association of human herpesvirus 6 infection with drug reaction with eosinophilia and systemic symptoms. *Arch. Dermatol.* 2001; **137**: 301–4.

11 Aihara M, Sugita Y, Nagatani T *et al.* Anticonvulsant hypersensitivity syndrome associated with reactivation of cytomegalovirus. *Br. J. Dermatol.* 2001; **144**: 1231–4.

12 Tanaka N, Kimura H, Hoshino Y *et al.* Monitoring four herpesviruses in unrelated cord blood transplantation. *Bone Marrow Transplant.* 2000; **26**: 1193–7.

13 Cook EB, Stahl JL, Lowe L *et al.* Simultaneous measurement of six cytokines in a single sample of human tears using microparticle-based flow cytometry: allergics vs. non-allergics. *J. Immunol. Methods* 2001; **254**: 109–18.

14 Hayashibara H, Tanimoto K, Nagata I, Harada Y, Shiraki K. Normal levels of IgG subclass in childhood determined by a sensitive ELISA. *Acta Paediatr. Jpn* 1993; **35**: 113–17.

15 Galindo Bonilla PA, Romero Aguilera G, Gomez Torrijos E *et al.* Phenytoin hypersensitivity syndrome with positive patch test. A possible cross-reactivity with amitriptyline. *J. Investig. Allergol. Clin. Immunol.* 1998; **8**: 186–90.

16 Yawalkar N, Shrikhande M, Hari Y, Nievergelt H, Braathen LR, Pichler WJ. Evidence for a role for IL-5 and eotaxin in activating and recruiting eosinophils in drug-induced cutaneous eruptions. *J. Allergy Clin. Immunol.* 2000; **106**: 1171–6.

17 Aihara Y, Ito S, Kobayashi Y, Aihara M. Stevens–Johnson syndrome associated with azithromycin followed by transient reactivation of herpes simplex virus infection. *Allergy* 2004; **59**: 118.
18 Yoshikawa T, Asano Y, Akimoto S *et al.* Latent infection of human herpesvirus 6 in astrocytoma cell line and alteration of cytokine synthesis. *J. Med. Virol.* 2002; **66**: 497–505.
19 Flamand L, Gosselin J, Stefanescu I, Ablashi D, Menezes J. Immunosuppressive effect of human herpesvirus 6 on T-cell functions: suppression of Interleukin-2 synthesis and cell proliferation. *Blood* 1995; **85**: 1263–71.
20 van Ginneken EEM, van der Meer JWM, Netten PM. A man with a mysterious hypogammaglobulinemia and skin rash. *Nether J. Med.* 1999; **54**: 158–62.
21 Horneff G, Lenard HG, Wahn V. Severe adverse reaction to carbamazepine: significance of humoral and cellular reactions to the drug. *Neuropediatrics* 1992; **23**: 272–5.
22 Ibia EO, Schwartz RH, Wiedermann BL. Antibiotic rashes in children: a survey in a private practice setting. *Arch. Dermatol.* 2000; **136**: 849–54.

See related Commentary on page v

Expression Profiling and Cellular Localization of Genes Associated with the Hair Cycle Induced by Wax Depilation

Yumiko Ishimatsu-Tsuji, Osamu Moro, and Jiro Kishimoto
Shiseido Life Science Research Center, Fukuura, Kanazawa-ku, Yokohama, Japan

The hair cycle is a highly regulated process controlled by multiple factors. Systematic analysis of gene expression patterns in each stage of the hair cycle would provide information useful for understanding this complicated process. To identify genes associated with the hair cycle, we used DNA microarray hybridization to analyze sequential gene expression patterns in mouse skin following hair cycle synchronization by wax depilation. Messenger RNA levels in mouse skin at various times after depilation were compared with those prior to depilation (resting phase). According to their expression patterns, upregulated genes were categorized into four groups: early anagen, middle anagen, late anagen/early catagen, and middle/late catagen, and processes that take place in each stage were evaluated. We identified 12 new components that are specifically expressed in the hair follicle, 11 genes in anagen including carbonic anhydrase 6, cytokeratin 12, and matrix metalloproteinase-11 in catagen that were confirmed using *in situ* hybridization. The strategy used here allowed us to identify unknown genes or process previously not suspected to have a role in hair biology. These analyses will contribute to elucidating the mechanisms of hair cycle regulation and should lead to the identification of novel molecular targets for hair growth and/or depilation agents.

Key words: DNA microarray sequence analysis/gene expression profiling/hair follicle/*in situ* hybridization
J Invest Dermatol 125:410–420, 2005

The hair cycle is a highly regulated process. Three phases have been defined in the mammalian hair cycle: anagen (growing phase), catagen (regressing phase), and telogen (resting phase) (Kligman, 1959). Intensive investigations have revealed the involvement of numerous genes that regulate the hair cycle, such as growth factors, adhesion molecules, cytokines, hormones, neuropeptides, and transcription factors (for reviews, see (Stenn and Paus, 2001)). But, in order to elucidate the complete picture of the molecular mechanisms involved and to understand the regulation of the hair cycle, many additional undiscovered molecules and pathways need to be characterized.

Recently, multiple aspects in the hair follicle have been guided by systematic analyses, including differential display, macroarray, and microarray analysis. DNA microarray has emerged as one of the most powerful approaches for systematic analysis, which detects changes in the expression of large numbers of genes. Using this method, several genes and metabolic processes were revealed to function in the hair follicle, such as GATA-3 in the cell fate decision of hair follicle morphogenesis (Kaufman *et al*, 2003), the defense response in alopecia areata (Carroll *et al*, 2002), or epithelial stem cell-specific genes (Morris *et al*, 2004; Tumbar *et al*, 2004).

Abbreviations: AAT, α-1 antitrypsin; eIF5A, eukaryotic translation initiation factor 5; EST, expressed sequence tag; LEF-1, lymphoid enhancer factor-1; MMP, matrix metalloproteinase; PABP, poly-A-binding protein; RT-PCR, reverse transcriptase polymerase chain reaction; TSP-1, thrombospondin 1

In this study, in order to identify genes involved throughout the hair cycle, we analyzed the sequential gene expression pattern of mouse skin that had its hair cycle synchronized by depilation. Taking advantage of DNA microarray hybridization, the messenger RNA (mRNA) levels in mouse skin at days 1, 3, 6, 13, 19, 21, and 23 after depilation were compared with genes expressed in skin without depilation. We focused on genes that were upregulated greater than 5-fold after hair induction, categorized them into four groups, early anagen, middle anagen, late anagen/early catagen, and middle/late catagen, and evaluated the processes that may take place in each stage. Moreover, we identified 12 new genes that are expressed specifically in the differential stage of hair follicle using *in situ* hybridization analysis and reverse transcription PCT.

Results

We used C57BL/6 mice that had their second hair cycle synchronized into the anagen induction phase by wax depilation at 8 wk of age. Figure 1 shows the morphology of hair follicles at each time point. At days 3 and 6, epithelium thickening was observed. At days 13 and 19, the formation of the hair shaft was complete and elongation had occurred. At day 21, typical morphologies of catagen, such as epithelial strand and trailing connective tissue sheath, were observed. According to the classification of hair cycle stages in mice (Muller-Rover *et al*, 2001), day 1 mainly includes anagen I hair follicles, day 3: anagen II, day 6: anagen III,

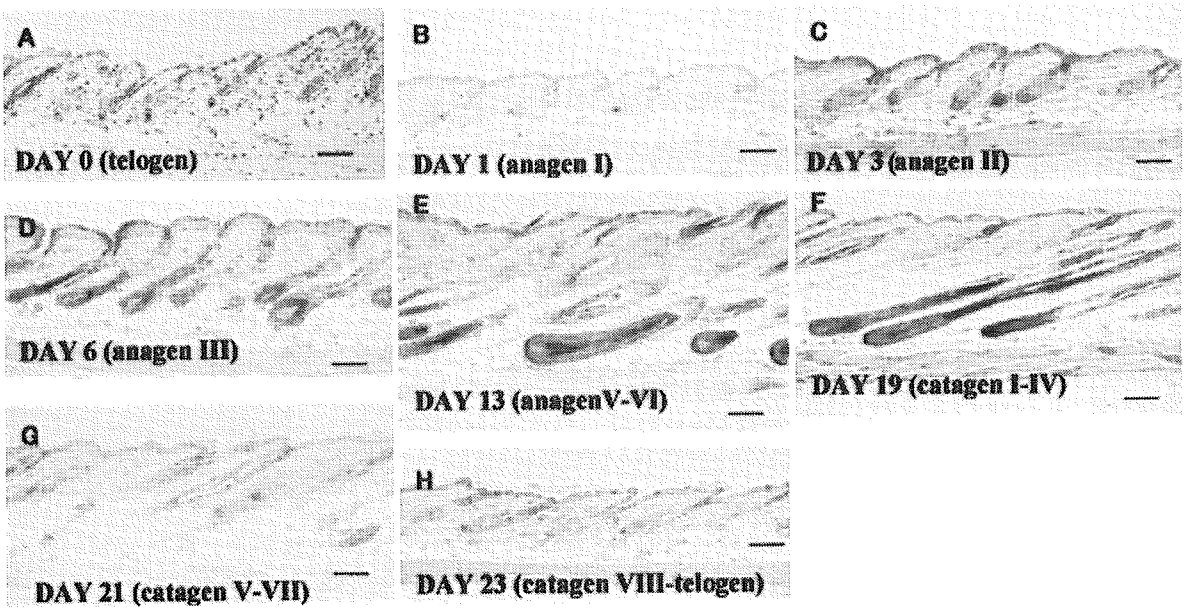

Figure 1
Sequential changes in hair follicle morphology after wax depilation. Days indicate the day after depilation. Day 0 indicates telogen hair before depilation. *Scale bar*: 100 μm.

day 13: anagen V–VI, day 19: catagen I–IV, day 21: catagen V–VII, and day 23: catagen VIII–telogen.

In order to analyze the molecular behavior in each stage of the hair cycle, gene expression of the total skin from mice taken at sequential time points after depilation (days 1, 3, 6, 13, 19, 21, and 23) was analyzed by DNA microarray hybridization and was compared with telogen (day 0) skin. Total skin taken from mice just before depilation (day 0) was used as a control.

To obtain the complete picture of changes in gene expression during the hair cycle, the results of representative microarray experiments at each time point are shown in log/log scatter plots (Fig S1). Upregulated genes at each time point are defined by the upper boundary lines at 2-, 3-, 5-, and 10-fold. Genes upregulated more than 2- or 3-fold were observed from day 1, the very early stage after depilation. At days 13 and 19 (Fig S1*D*, *E*), genes significantly upregulated more than 10-fold were observed, and a greater number of genes were upregulated compared with the other times examined. At day 23, changes had almost converged back to the baseline control (Fig S1*G*).

Table I shows the percentage and absolute number of genes upregulated reproducibly in duplicate microarrays greater than 2-, 3-, 5-, and 10-fold at each time point. The number of genes that had detectable and reproducible signals was not significantly different at each time point. Correlation coefficients (r) between duplicate chips at the same time points were calculated, and the data for genes elevat-

Table I. Percentage of upregulated genes at each time point after depilation

	Day 1		Day 3		Day 6		Day 13		Day 19		Day 21		Day 23	
2-fold	107	(1.4)[a]	147	(1.9)	123	(1.7)	443	(5.8)	668	(9.1)	55	(0.7)	16	(0.2)
3-fold	31	(0.4)	37	(0.5)	30	(0.4)	157	(2.1)	281	(3.8)	19	(0.3)	4	(0.1)
5-fold	9	(0.1)	9	(0.1)	7	(0.1)	51	(0.7)	79	(1.1)	11	(0.1)	0	(0.0)
(First exp)	24	(0.3)	17	(0.2)	69	(0.9)	121	(1.6)	88	(1.2)	14	(0.2)	4	(0.1)
(Second exp)	18	(0.2)	42	(0.6)	83	(1.1)	146	(1.9)	182	(2.5)	17	(0.2)	10	(0.1)
10-fold	1	(0.0)	1	(0.0)	1	(0.0)	24	(0.3)	24	(0.3)	6	(0.1)	0	(0.0)
Total genes detected[b]	7395		7556		7443		7603		7344		7364		7010	
Correlation coefficient[c]	0.69		0.44		0.26		0.82		0.86		0.73		0.11	

Exp, experiment.
[a]Absolute number of genes up-regulated reproducibly is in blacket.
[b]Correlation coefficient between duplicate microarray experiments.
[c]The number of genes that had a detectable signal reproducibly.
The signal value was calculated as the ratio between the signal intensity of the experimental data to the control (day 0 Telogen mice before wax depilation) data.

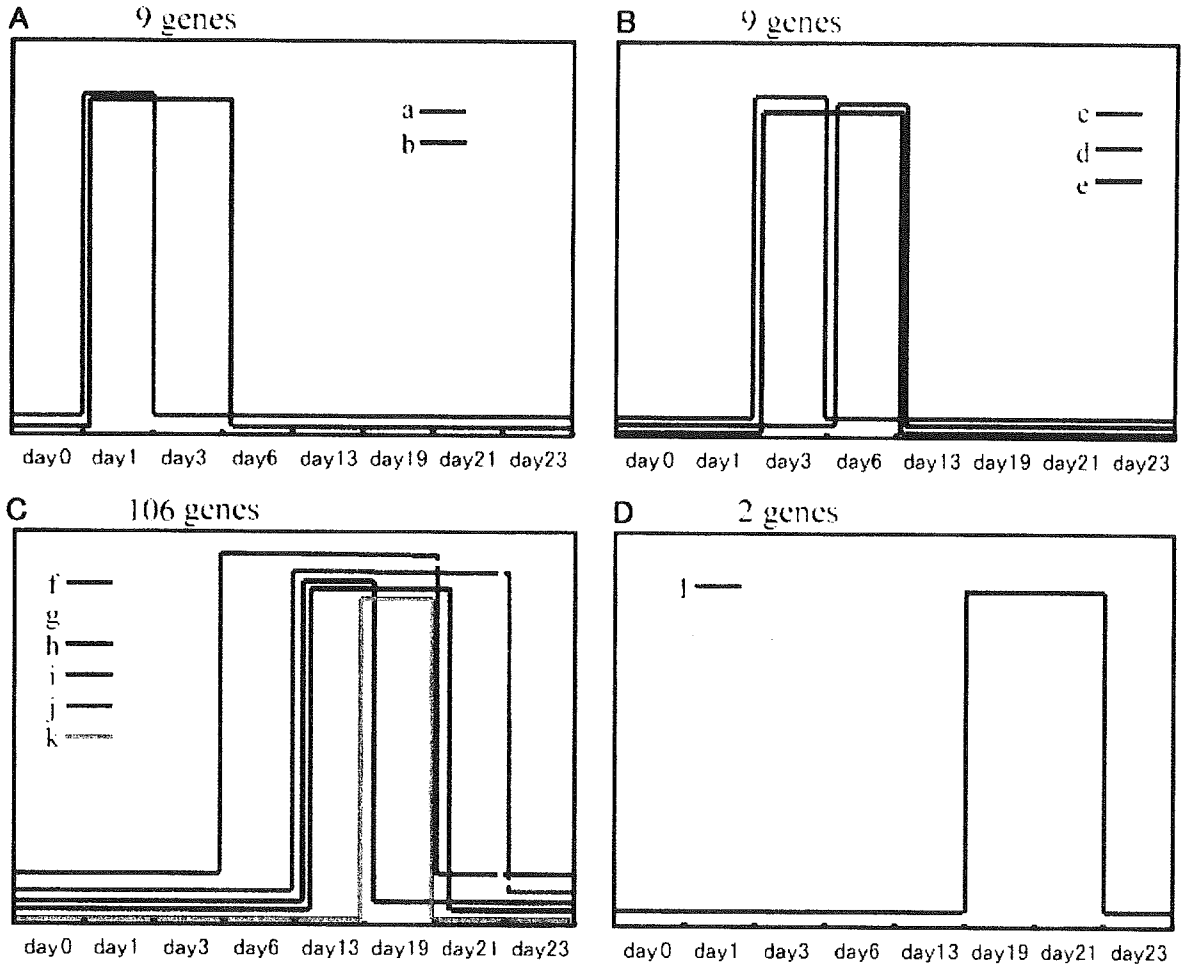

Figure 2
Grouping of upregulated genes with similar expression patterns. Genes upregulated greater than 5-fold were grouped into 12 groups (*a–l*) according to their expression patterns. Each group was classified further into four classes. (*A*) Early anagen (including groups *a–b*); (*B*) middle anagen (including groups *c–e*); (*C*) late anagen/early catagen (including groups *f–k*); and (*D*) middle/late catagen (including group *l*).

ed 5-fold in each experiment were obtained. The duplicate data were significantly correlated at days 1 and 3, and were highly significantly correlated at days 13, 19, and 21. At day 6, a weak correlation was observed, which is likely because of the drastic changes in the hair cycle during this period so that a mixed population of follicles at slightly different stages coexists at this period. Consistent with the overview shown in Fig S1, many genes were upregulated at days 13 and 19. At day 23, the transcripts fell within the 5-fold limits, which might cause poor correlation ($r<0.2$) of duplicated data.

We selected genes upregulated greater than 5-fold to analyze in further detail. Most genes shown in Table I were elevated at multiple time points. To characterize the expression profiling of each gene in the hair cycle, upregulated genes at each time point were classified into 12 groups named such as group a-l, by their expression patterns (Fig 2). Furthermore, each group was assigned to one or more hair cycle stages, considering the morphology of the hair follicle, as follows: "Early anagen" includes groups a–b, in which the gene expression was upregulated at day 1; "middle anagen" includes groups c–e, in which the gene expression was upregulated at days 3 or 6 and with no change at days 1 and 13; "late anagen and early catagen" includes groups f–k, upregulated at days 13 or 19; and "middle and late catagen" includes group l, upregulated at day 21 and with no change at day 13.

Table II show transcripts that were upregulated in early anagen, middle anagen, late anagen/early catagen, and middle/late catagen, respectively (A complete list of the genes upregulated in late anagen and early catagen is supplied as Table S2). The numbers in the tables show the average of fold-change of the two identical array experiments. In late anagen, a substantial number of genes (106 genes) were included (Table S1). To elucidate processes that take place during the formation of the hair follicle, genes were classified according to their biological function. The 106 genes were sorted into 14 functional groups, transcription, translation, cell communication, cell adhesion, signal transduction, axon guidance, transport, cytoskeleton, ubiquitin cycle, defense response, metabolism, or others/unknown, according to the biological process category or molecular function category of the National Center for Biotechnology Information (NCBI) Gene Ontology database.

Table II. Genes upregulated in each specific period and fold-change during hair cycle

Gene name	Gene no.	Unigene	Day 1	Day 3	Day 6	Day 13	Day 19	Day 21	Day 23	Group	
Early anagen											
Lipocalin 2	AA087193	Mm.9537	18.2	2.0	1.0	0.6	ND	0.9	0.8	a (a[a])	O
Small inducible cytokine A2	AI323202	Mm.145	10.1	3.5	1.0	0.8	0.6	2.0	1.4	a	
Schlafen 4	AI646186	Mm.38192	10.7	1.3	2.8	0.9	0.7	1.4	3.3	a	O
Ankyrin repeat domain 1 (cardiac muscle)	AA792499	Mm.10279	7.2	4.7	1.0	0.9	1.5	1.2	0.8	a	O
Secretory leukocyte protease inhibitor/antileukiproteinase 1 precursor	AI020539	Mm.1395	8.7	2.4	3.6	1.4	1.9	1.9	1.1	a	
Cardiac morphogenesis	AA501052	Mm.10117	7.4	1.1	1.3	0.6	1.4	0.6	0.8	a	O
S100 calcium-binding protein A9/calgranulin B	AA255025	Mm.2128	8.9	3.1	1.4	1.1	1.4	1.1	1.1	a	
Chemokine (C–C motif) ligand 7/small inducible cytokine A7/Monocyte chemotactic protein 3	AA711435	Mm.16091	8.3	3.5	0.7	0.8	0.6	1.8	3.9	a	
Tissue inhibitor of metalloproteinase 1	AA184223	Mm.8245	10.8	7.2	4.2	1.0	1.1	1.6	1.9	b	N
Middle anagen											
Baculoviral inhibitor of apoptosis (IAP) repeat-containing inhibitor survivin	AA671290	Mm.8552	3.8	6.2	5.3	3.6	ND	ND	1.4	c	
CDK5 regulatory subunit-associated protein 2	AI605614	Mm.39965	3.9	9.9	5.5	2.8	2.9	2.0	1.3	c	
Ars component B	W20775	Mm.27630	4.2	10.5	4.1	1.8	1.0	1.6	2.5	c	O
Cell division cycle-associated 3/gene-rich cluster, C8 gene/a trigger of mitotic entry	AA416441	Mm.22228	4.1	6.8	4.9	6.4	2.9	1.2	2.0	c	
Shc SH2-domain-binding protein 1	AW210261	Mm.37801	ND	12.2	7.2	ND	ND	1.5	1.6	c	N
Kinesin family member C1	AA003218	Mm.197684	4.9	7.1	8.5	5.2	2.4	1.6	1.4	c	N
Small proline-rich protein 2A	AI605648	Mm.6853	ND	39.2	27.1	5.2	ND	ND	1.9	d (d[a])	
Spectrin β2	AA871274	Mm.31326	2.8	9.3	17.2	2.2	1.6	2.3	1.3	d	N
Retinol-binding protein 2, cellular	AI385457	Mm.12825	3.3	3.0	6.3	2.1	1.4	1.8	1.2	e	O
Late anagen and early catagen											
Keratin complex 1, acidic, gene 12	AA684158	Mm.4201	2.4	1.5	1.2	3.7	11.6	1.5	1.2	k	H
Keratin-associated protein 3–3	NM_025524	Mm.30539	0.9	1.2	7.7	100.0	100.0	14.5	3.2	g (i[a])	H
EST similar to keratin-associated protein	AA763224	Mm.69020	0.6	ND	ND	34.7	70.4	11.1	2.2	j (j[a])	H
RIKEN cDNA 4733401H21gene/EST similar to keratin-associated protein	AA067279	0	0.8	ND	ND	57.3	65.2	1.8	1.7	i (i[a])	H
Poly-A-binding protein, cytoplasmic 1	NM _008774	Mm.321828	1.1	1.6	ND	12.1	ND	ND	ND	h (h[a])	H
Eukaryotic translation initiation factor 5	AA399766	Mm.196607	1.8	2.4	4.7	18.1	12.4	1.3	0.9	i (i[a])	H
Cytidine 5′-triphosphate synthase	AA185252	Mm.1815	2.0	2.3	2.5	7.0	11.3	0.9	0.8	i	H
Carbonic anhydrase 6	AA760185	Mm.232523	0.6	1.2	2.8	85.3	62.7	14.3	2.2	j (j[a])	H
Cathepsin E	AA839435	Mm.230249	1.4	1.1	2.2	12.8	4.4	1.4	1.2	h	H
RIKEN cDNA 1810008K03 gene	AI390168	Mm.35083	ND	0.8	1.8	14.7	21.5	2.2	1.4	i (i[a])	H
High-glycine/tyrosine protein type I E5 mRNA	NM_133359	Mm.188445	ND	1.9	ND	100.0	100.0	31.6	3.4	j (j[a])	H
Early catagen											
Thrombospondin 1	AI180914 2	Mm.4159	1.6	2.3	1.3	2.2	20.0	7.5	2.8	l (k[a])	
Matrix metalloproteinase 11	AI120903	Mm.4561	0.7	0.5	0.7	ND	5.9	10.2	ND	l	H

Listed only upregulated genes that show *in situ* signals in hair follicles. Complete list is supplied in supplemental data as Table S2.
O, detected in other areas in the skin; N, no signal was detected; H, detected in hair follicle; EST, expressed sequence tag; cDNA, complementary DNA; mRNA, messenger RNA; IAP, inhibition of apoptosis; ND, not defined.
[a]Upregulated greater than 10-fold reproducibly.

In cases where the gene has several functions, we refer to the function for which the gene is best known.

In order to confirm the hair follicle-specific expression of these genes, mRNA localization was analyzed by *in situ* hybridization. We preferentially selected 45 genes whose localization in the hair follicle had not been previously reported. Localization of signals for those 45 genes are marked with "H," "O," and "N" in Table II. As a result, 12 newly identified genes gave detectable signals in the hair follicle (Table III). In addition, Clusterin, which was previously reported in the hair follicle (Seiberg and Marthinuss, 1995), was also detected. Seventeen genes were detected in the skin other than hair follicles, perhaps in putative mast cells, nerves, vessels, and/or fibroblasts in the dermis. No signal was detected at all for 15 genes.

Figure 3 shows the results of *in situ* hybridization of 11 genes upregulated in late anagen using paraffin sections of mouse skin at day 13 after depilation. Carbonic anhydrase 6 was expressed in the outer root sheath above the boundary of the dermis and subcutis. Cytidine 5′-triphosphate synthase was expressed in the cuticle below the boundary of the dermis and subcutis. Cathepsin E was expressed in the cuticle of the keratogenous zone. Poly-A-binding protein (PABP)/cytoplasmic 1 (Sachs *et al*, 1986; Afonina *et al*, 1998; Deo *et al*, 1999) and eukaryotic translation initiation factor 5 (eIF5A) (Nishimura *et al*, 2002) were expressed in germinative hair matrix cells. Cytokeratin 12 was detected in the inner root sheath of the hair bulb. In the cortex, keratin-associated protein 3-3, expressed sequence tag (EST) AA763224, high-glycine/tyrosine protein type I E5 mRNA, Riken complementary DNA (cDNA) 4733401H21, and Riken cDNA 1810008K03 were detected (Fig 3*G–K*). The signals for KAP 3-3 and Riken cDNA 1810008K03 were detected in more restricted areas of the cortex than EST AA763224 and high-glycine/tyrosine protein type I E5 mRNA. The localization of Riken cDNA 4733401H21 was in a characteristic manner, showing an asymmetric expression pattern and expression only in the skin surface side of the cortex.

To confirm the differential expression of newly identified genes, we analyzed the expression of genes at different stages of the hair cycle by quantitative PCR. Eleven of 12 genes that were identified in the hair follicle by *in situ* hybridization at day 13 were upregulated remarkably in anagen by reverse transcriptase polymerase chain reaction (RT-PCR) (Fig 4*A*). Furthermore, we analyzed stage specificity by *in situ* hybridization. Fig 4*B–D* shows representative differential expression data of keratin 3–3, cytokeratin 12, and carbonic anhydrase 6. Only cytokeratin 12 was detected, not only in late anagen but also in telogen; however, the signal-detected area was remarkably restricted in telogen, which is consistent with the microarray results.

In catagen, the expression and localization of matrix metalloproteinase (MMP)-11, which is known to be a unique member of the MMP family (Murphy *et al*, 1993), was analyzed. Figure 4*A*-No. 12 shows the specific expression of MMP-11 at catagen and telogen by RT-PCR. Figure 5 shows the staining of MMP-11 in anagen and catagen hair follicles by *in situ* hybridization. The signal was detected in the trailing connective tissue sheath of catagen hair follicles. No signals were observed in anagen in contrast to catagen.

Discussion

Overview In this study, we analyzed the sequential changes of gene expression patterns that occur throughout the hair

Table III. Genes detected in hair follicle by *in situ* hybridization

	Experiment 1			Experiment 2				
	Expression value			Expression value				
Gene name	Control[a]	Sample[b]	Ratio	Control[a]	Sample[b]	Ratio	Localization	Stage
Carbonic anhydrase 6	299	33,217	>100[c]i>	604	42,682	70.7	ORS	Late anagen
Cytidine 5′-triphosphate synthase	391	2095	5.4	653	5678	8.7	Cuticle	Late anagen
Cathepsin E	573	4215	7.4	501	9180	18.3	Cuticle	Late anagen
Poly A-binding protein, cytoplasmic 1	166	1672	10.1	124	1745	14.0	Matrix	Late anagen
Eukaryotic translation initiation factor 5	611	14,968	24.5	2628	30,646	11.7	Matrix	Late anagen
Cytokeratin 12	517	1137	2.2	359	1849	5.1	IRS	Late anagen
Keratin-associated protein 3–3	508	68,736	>100[c]	410	79,222	>100[c]	Cortex	Late anagen
EST AA763224 gene	142	72,401	>100[c]	111	95,502	>100[c]	Cortex	Late anagen
High-glycine/tyrosine protein type I E5	265	43,613	>100[c]	287	131,564	>100[c]	Cortex	Late anagen
Riken cDNA 4733401H21 gene	46	2989	65.2	67	3322	49.4	Cortex	Late anagen
Riken cDNA 1810008K03 gene	515	5642	10.9	847	15,564	18.4	Cortex	Late anagen
MMP-11	683	7898	11.6	224	1970	8.8	CTS	Catagen

MMP, matrix metalloproteinase; ORS, outer root sheath; IRS, inner root sheath; EST, expressed sequence tag; cDNA, complementary DNA; CTS, connective tissue sheath.
[a]Expression value at day 0.
[b]Expression value at day 13 for all genes except MMP-11 or day 21 for MMP-11.
[c]Defined "more than 100-fold" by Feature Extraction Software.

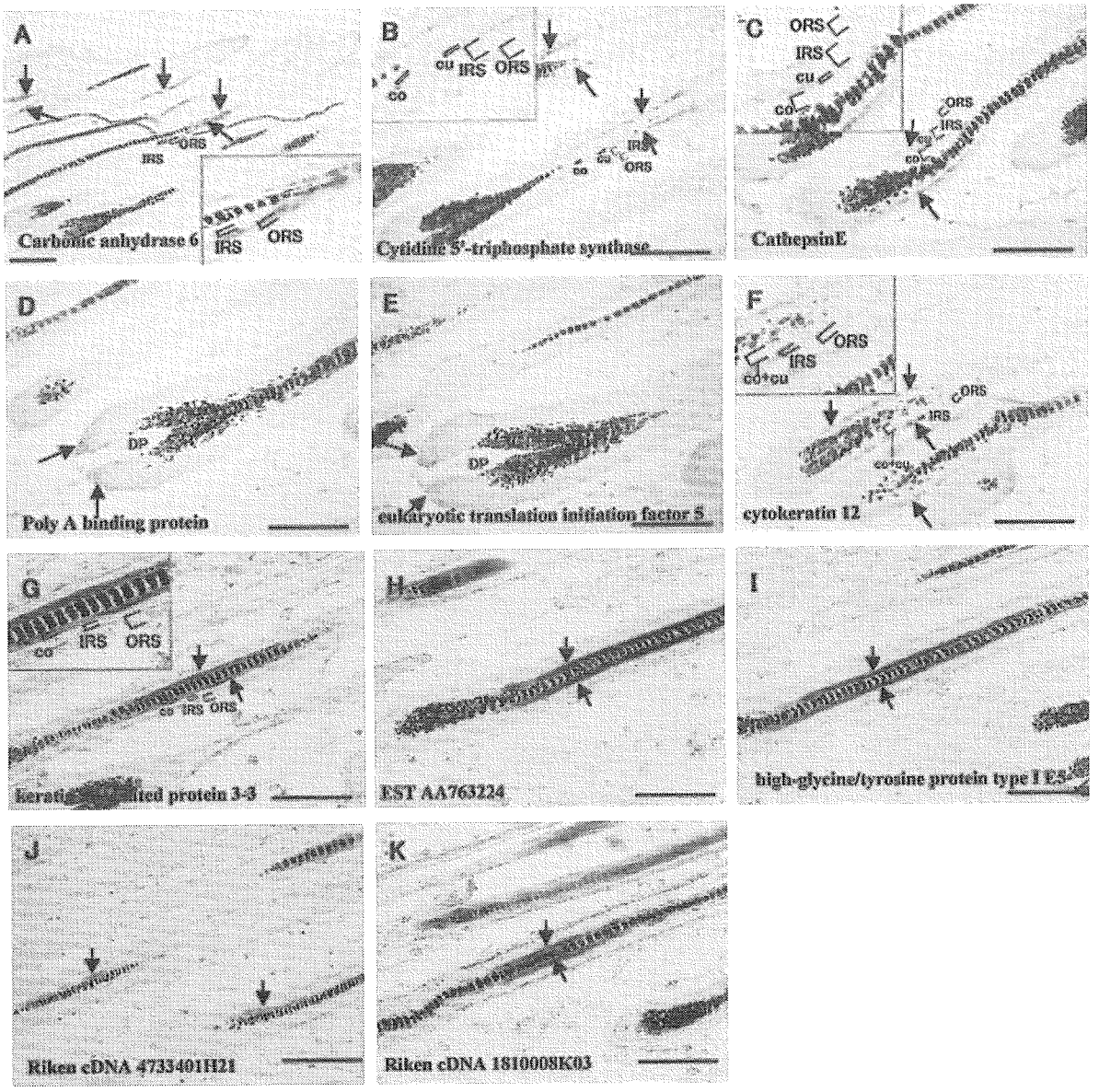

Figure 3
The localization of genes upregulated in late anagen. (*A*) Carbonic anhydrase 6; dotted line indicates the boundary of the dermis and subcutis. (*B*) cytidine 5′-triphosphate synthase. (*C*) cathepsin *E*; (*D*) poly-A-binding protein, cytoplasmic 1; (*E*) eukaryotic translation initiation factor 5; (*F*) cytokeratin 12; (*G*) keratin-associated protein 3–3; (*H*) expressed sequence tag (EST) AA763224; (*I*) high-glycine/tyrosine protein type I E5; (*J*) Riken cDNA 4733401H21; and (*K*) Riken cDNA 1810008K03. Arrows indicate the signals. Magnified views are shown in the insets. co, cortex; cu, cuticle; IRS, inner root sheath; ORS, outer root sheath; DP, dermal papilla; cDNA, complementary DNA; EST, expressed sequence tag. *Scale bars*: 100 μm.

cycle using DNA microarray hybridization. We identified genes upregulated more than 5-fold at each time point of the hair cycle and assigned them to four hair cycle stages: (I) early anagen, (II) middle anagen, (III) late anagen/early catagen, and/or (IV) middle/late catagen. Exploiting this list, we could hypothesize processes that take place in each stage of the hair cycle caused by physical stimulation,as follows: (I) just after depilation: defense response or defense response-related processes; (II) at 3 or 6 d after depilation: keratinocyte proliferation-related processes; (III) late anagen and early catagen: multiple processes including keratin intermediate filament formation; and (IV) middle and late catagen: processes that include MMP-11 or thrombospondin (TSP)-1. On the basis of these lists, we identified 12 novel components of the hair follicle that had not been previously suspected to play a role in hair biology, and confirmed their expression using *in situ* hybridization analysis. The novel components identified were mainly specific for late anagen or early catagen. Considering the fact that dynamic growth of the hair follicle takes place at this time, the strategy we employed here, in which total skin was used for starting material and mRNA from hair follicle cells only represents a fraction of the total mRNA analyzed on the cDNA gene chips, may be suitable to identify genes that directly function in the construction or elongation of the hair follicle. Recently, Lin *et al* (2004) reported the identification of hair cycle-associated genes

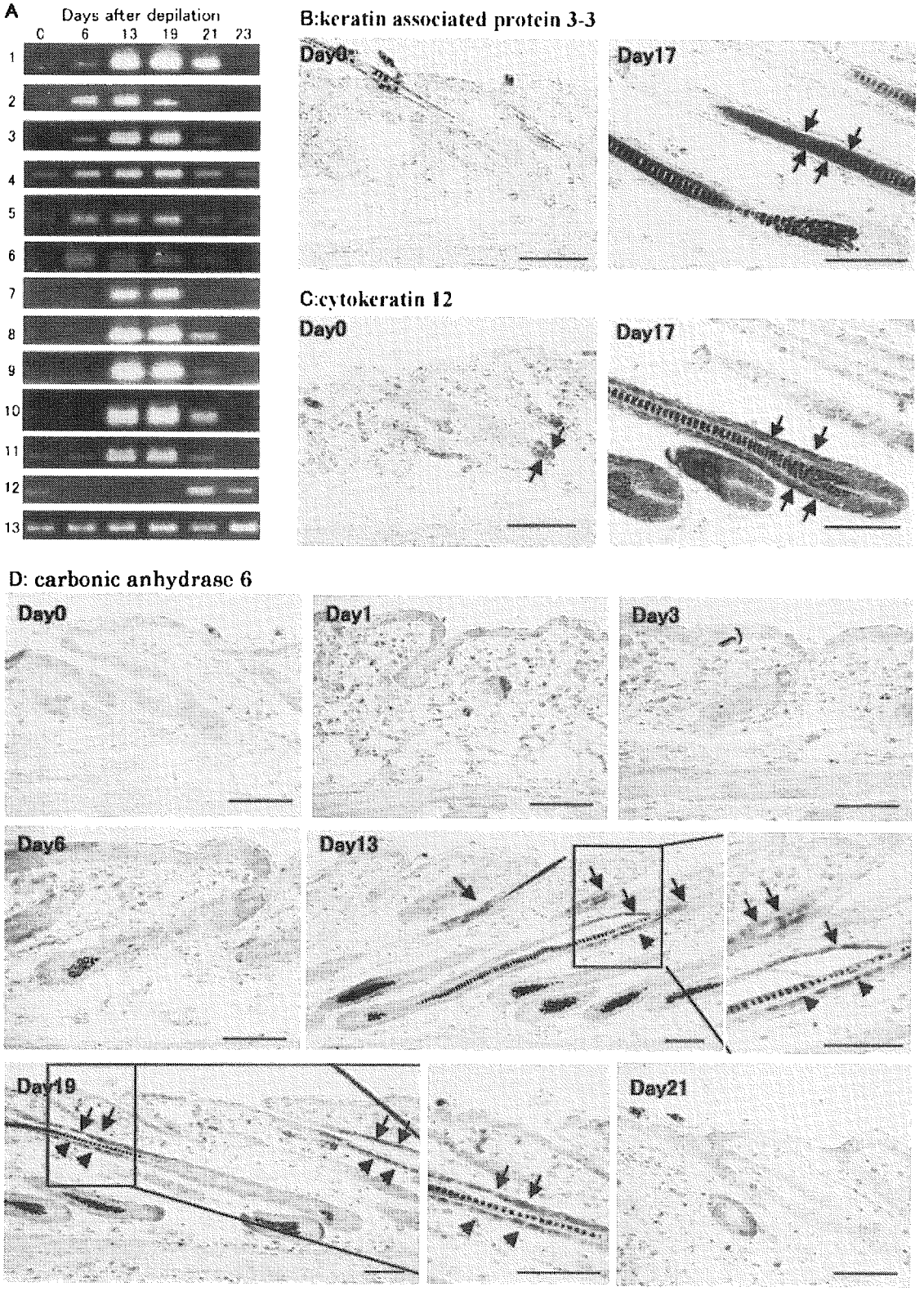

Figure 4
Differential expression of the microarray-identified genes during the hair cycle. (*A*) Semiquantitative RT-PCR. *1*, carbonic anhydrase 6; *2*, cytidine 5′-triphosphate synthase; *3*, cathepsin E; *4*, poly-A-binding protein, cytoplasmic 1; *5*, eukaryotic translation initiation factor 5; *6*, cytokeratin 12; *7*, keratin-associated protein 3–3; *8*, EST AA763224; *9*, high-glycine/tyrosine protein type I E5; *10*, Riken cDNA 4733401H21; *11*, Riken cDNA 1810008K03; *12*, MMP-11; *13*, GAPDH. (*B*, *C*) Expression of cytokeratin 12 (*B*) and keratin-associated protein 3-3 (*C*) in telogen (day 0 without wax depilation) and anagen (day 17 after wax depilation) was analyzed by *in situ* hybridization. (*D*) Sequential change of carbonic anhydrase 6 expression during the hair cycle was analyzed by *in situ* hybridization. Note that the signal intensity of cytokeratin 12 in C was overexposed with automated processing system compared with Fig 3*F*. *Scale bar*: 100 μm. EST, expressed sequence tag; GAPDH, glyceraldehyde-3-phosphate dehydrogenase; RT-PCR, reverse transcriptase polymerase chain reaction; MMP, matrix metalloproteinase.

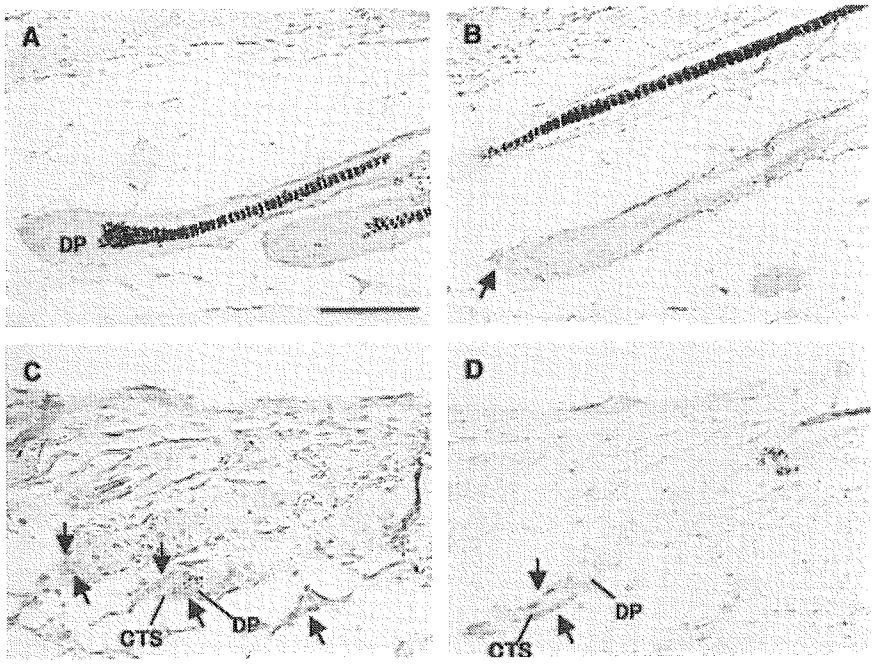

Figure 5
Localization of MMP-11 in catagen. Localization of MMP-11 during catagen was analyzed by *in situ* hybridization (*A–D*). (*A*) Late anagen; (*B*) early catagen; (*C*) middle catagen; and (*D*) late catagen. Arrows indicate the signals. MMP, matrix metalloproteinase; CTS, connective tissue sheath; DP, dermal papilla. *Scale bars*: 100 μm.

by DNA microarray. They reported several genes expressed at each hair cycle stage, which are consistent with our microarray results, such as hair keratins and hair-keratin associated genes, carbonic anhydrase, and neuroblastoma myc-related oncogene 1. On the other hand, other differences between their study and ours may be because of multiple factors, including differences in DNA microarray chips used (Agilent cDNA array *vs* Affymetryx oligo array), hair cycle models (wax depilation *vs* natural hair cycle), and/or analytical methods (fold-changes *vs* clustering). Therefore, in order to confirm the significant expression of genes from these experimental array data, confirmation of hair follicle specific or follicle-associated gene expression by *in situ* hybridization seems to be crucial, as we performed for our 11 newly identified genes.

Taking the results together, we consider each stage as follows:

Early and middle anagen Six of the eight genes on the early anagen list could contribute to inflammation, such as lipocalin 2, schlafen 4, secretory leukocyte protease inhibitor, S100 calcium-binding protein A9 (calgranulin B), chemokine (C–C motif) ligand 7, and tissue inhibitor of metalloproteinase (Table II). These observations suggest that two processes, anagen induction and inflammatory or regenerative responses to damaged epithelia, take place in this stage.

Four of eight genes on the middle anagen list (Table II) could function in cell proliferation, such as cell division cycle-associated 3, Shc SH2-domain-binding protein 1, kinesin family member C1, and baculoviral inhibitor of apoptosis (IAP) repeat-containing 5. Two genes related to keratinocyte differentiation, Small proline-rich protein 2A and retinol-binding protein 2, are also included in this list. Cell cycle and differentiation-related genes on the list might contribute to keratinocyte proliferation during epithelium thickening, which is markedly observed at day 3 and especially at day 6 (Fig 1*C*, *D*).

Late anagen and early catagen A substantial number of genes already reported to play some role in the hair follicle are on this list (Tables II and S1). Components of keratin intermediate filaments and EST of putative keratin-associated proteins, which contribute to the structure of hair fibers, were highly upregulated more than 10-fold. Besides keratin-related proteins, lymphoid enhancer factor (LEF)-1, forkhead box N1, and vitamin D receptor are also on that list. These proteins had been reported to be crucial for the hair cycle according to *in vivo* analysis by gene targeting or overexpression in a transgenic model (DasGupta and Fuchs, 1999; Hong *et al*, 2001; Kong *et al*, 2002). These facts suggest that other genes included in Table II could play important roles in the hair follicle. Other genes on the list could have functions in the hair cycle, as follows:

Catalytic enzymes Cytidine 5′-triphosphate synthase plays a role in the biosynthesis of nucleic acids and membrane phospholipids (Ostrander *et al*, 1998; Hatse *et al*, 1999), and cathepsin E, an endolysosomal aspartic proteinase, is known to be predominantly expressed in immune system cells. Besides lymphoid tissues, cathepsin E is distributed in multiple tissues and cell types, such as the gastrointestinal tract, blood cells, and microglia (Nakanishi *et al*, 1993; Ikuzawa *et al*, 2003). Carbonic anhydrase 6, a zinc-containing enzyme, is known to be secreted in saliva and regulates oral pH (Kivela *et al*, 1999). Recently, the morphogenetic roles of carbonic anhydrase 6 in taste bud growth (Thatcher *et al*, 1998) and in development of the infant alimentary tract (Karhumaa *et al*, 2001) have been reported. Moreover, carbonic anhydrase 6 has been suggested to contribute to taste dysfunction resulting from zinc deficiency (Goto *et al*, 2000) and alopecia, which also results from severe zinc deficiency (Prasad, 1988). It is possible that carbonic anhydrase 6 and two other catalytic enzymes play roles in keratinocyte differentiation in the hair follicle as in

other tissues. A recent report by Lin *et al* (2004) also showed late anagen and early catagen expression of carbonic anhydrase 6 in the natural murine hair cycle, which is consistent with our observations, and suggests its relation to apoptotic events.

Cell proliferation The detection of two cell proliferation-related genes, PABP/cytoplasmic 1 and eIF5A, in germinative matrix cells is also noteworthy. PABP recognizes the 3′ poly-A mRNA tail and plays critical roles in eukaryotic translation initiation and mRNA stabilization/degradation (Sachs *et al*, 1986; Afonina *et al*, 1998; Deo *et al*, 1999). Because its expression is elevated in growing cells, it has been implicated in cell proliferation (Gorlach *et al*, 1994). The gene product of eIF5A has also been implicated in cell viability and cell proliferation (Nishimura *et al*, 2002; Park *et al*, 2003). The hair matrix is considered to be occupied by "transient amplifying" cells that proliferate constantly during anagen (Paus *et al*, 1994; Xu *et al*, 2003). Thus, it is reasonable to assume that these two proteins participate in the proliferation of the hair matrix. Moreover, eIF5A is the only protein known to undergo hypusination, a unique post-translational modification for activation (Park *et al*, 2003). The regulation of hypusination could also be important in the anagen hair follicle.

Transcription in the hair cortex The identification of five genes (keratin-associated protein 3-3, EST AA763224, high-glycine/tyrosine protein type I E5, Riken cDNA 4733401H21, and Riken cDNA 1810008K03) in the hair cortex is also noteworthy. Expecting that these genes could be regulated by similar transcriptional mechanisms, we investigated transcription factor-binding sites in the 5′ upstream regions from −3000 to −1 of each gene in detail, except for EST AA763224, whose full-length cDNA has not yet been sequenced. As a result, the binding motifs of two transcription factors (LEF-1 and runx-1) are found in the 5′ upstream region of all five genes. LEF-1 is a well-known transcription factor that participates in regulating multiple keratin expression and is important for hair follicle patterning (Zhou *et al*, 1995). Although runx-1 is the most frequently translocated gene in human leukemia, and has not been previously reported to be involved with hair follicle formation, it could regulate transcription cooperatively with LEF-1 through recruitment of the co-repressor TLE1 (Levanon *et al*, 1998; Lutterbach *et al*, 2000). Interestingly, both LEF-1 and runx-1 are upregulated in late anagen and are also listed in Tables II and S1. It is possible that these two transcription factors may play important cooperative roles in hair cortex formation.

Eye components Cytokeratin 12, which is known to be a component of the corneal epithelia (Ferraris *et al*, 2000), was detected in the inner root sheath of the hair bulb. Suggestively, the expression of crystallin β A4 (which is the major component of the eye lens) and aquaporin 1 water channel (which is present in the ciliary body of the eye) (Patil *et al*, 2001) was also elevated in anagen (Tables II and S1). Corneal epithelium and epidermal keratinocytes are known to share a common embryological origin and to diverge reversibly during embryogenesis. In addition to their embryological identity, the hair follicle and cornea might share common properties even in adult tissues.

Middle and late catagen Only two genes, TSP-1 and metalloproteinase-11, were significantly increased in these stages. TSP-1 has been reported to play a critical role in the induction of hair follicle involution and in vascular regression during the catagen phase (Yano *et al*, 2003). MMP-11 is known to be a unique member of the MMP family, which is not directly involved in extracellular matrix degradation (Murphy *et al*, 1993). It had not been reported to be involved with the hair cycle, but it is expressed in tissues undergoing active remodeling associated with embryonic development, wound healing, and tumor invasion (Basset *et al*, 1990; Okada *et al*, 1997; Boulay *et al*, 2001). Its unique substrate specificity might be a clue to reveal its function. α-1 antitrypsin (AAT) and insulin-like growth factor-binding protein-1 have been identified as physiologic targets for MMP-11 (Pei *et al*, 1994; Manes *et al*, 1997). It is noteworthy that AAT is upregulated in anagen and is listed in Tables II and S1. It is possible that AAT plays some role in anagen, and its disappearance may be important during catagen progression. Recently, both MMP-11 and AAT were implicated in apoptosis (Daemen *et al*, 2000; Ishizuya-Oka *et al*, 2000; Hagglund *et al*, 2001). Apoptosis is an important process during the regression of the catagen hair follicle (Lindner *et al*, 1997; Soma *et al*, 2002). It could be speculated that MMP-11 expression in the trailing connective tissue sheath contributes to the regulation of epithelial regression. From these observations, the regulation of MMP-11 activity by 4- Abz- Gly- Pro- D- Leu- D- Ala- NH- OH (MMP inhibitor I) or by a specific inhibitor of MMP-11 (Matziari *et al*, 2004) or the regulation of its gene expression by all *trans*-retinoic acid, FGF2, insulin-like growth factor-II, epidermal growth factor, platelet-derived growth factor, interleukin-6, and/or 12-*O*-tetradecanoylphorbool-13-acetate (Anderson *et al*, 1995; Delany and Canalis, 1998; Singer *et al*, 1999) could have significant effects on the hair cycle.

Materials and Methods

Tissue preparation Female C57BL/6 mice (Charles River Laboratories, Atsugi, Japan), approximately 8 wk of age, were used for microarray and gene localization analysis, because the hair cycle is well characterized in this mouse strain (Muller-Rover *et al*, 2001). The hair cycle was synchronized on the dorsal skin by wax depilation as described previously (Yano *et al*, 2001). Pigmentation of the skin, which is the sign of hair induction, was observed from day 6 after depilation. Dorsal skin at days 1, 3, 6, 13, 19, 21, and 23 after depilation and at day 0, the day before depilation, was used. All animal procedures had the approval of the ethical committee of Shiseido Research Center.

Preparation of total RNA Total RNA was extracted as described previously (Wada *et al*, 2002). Briefly, after being euthanized, mice were shaved with mechanical clippers and total, full-thickness dorsal skin was dissected free. Underlying fascia and soft tissue were removed, and the skin was cut into small (0.5 cm) pieces and frozen quickly in liquid nitrogen. The frozen skin pieces were physically crushed with a Cryo-press apparatus (Microtec, Funabashi, Japan) for 45 s. Each powdered sample was dissolved in 1 mL ISOGEN (NIPPON GENE CO., LTD, Toyama, Japan), and total RNA was isolated. After RNA precipitation, RNA was purified using an RNeasy spin column system, according to the

manufacturer's instructions (Qiagen Inc., Valencia, California). Total RNA quality was assessed by recombinant RNA ratio [28S/18S] using an Agilent Bioanalyzer 2100 (Agilent Technologies, Palo Alto, California).

Microarray analysis Two experiments were performed, and the results of the two studies were statistically analyzed using two control–sample pairs of mice, a total of four mice for each time point. cDNA microarray analysis was performed according to the manufacturer's instructions (Agilent Technologies) as previously described (Seseke *et al*, 2004). Thirteen micrograms of total RNA was converted to fluorescently labeled cDNA by *in vivo* transcription using the Fluorescent direct label kit (Agilent Technologies) in the presence of oligo(dT) primer (5 μM), Moloney muria leukemia virus (MMLV)-reverse transcriptase (10 U), and CTP labeled with fluorescent dye. Fifty micromoles Cyanine 5-dCTP (Perkin-Elmer, Boston, Massachusetts) was used for samples from day 1, 3, 6, 13, 19, 21, and 23, and Cyanine 3-dCTP for the control from day 0. The resulting labeled cDNA of each sample and control were mixed and hybridization to the microarray on which 8720 genes are spotted (the mouse cDNA microarray: G4104A, Agilent Technologies) was performed overnight at 65°C. Microarray slides after hybridization were washed with 0.5 × SSC and 0.01% sodium dodecyl sulfate and then washed with 0.06 × SSC. After drying the slides, the fluorescence of bound cDNA on the microarrays was quantitated using a microarray scanner (Agilent dual-laser Microarray scanner G2565AA). The signals were analyzed using Feature Extraction Software (Agilent Technologies), excluding the data from signals that was recognized as outlier or equal to background. The signal value was calculated as the ratio between the signal intensity of the experimental data to the control data. Scattering of the ratios between duplicate experiments were calculated as correlation coefficients using statistical function "CORREL" with Microsoft Excel software.

***In situ* hybridization** *In situ* hybridization was performed on 4 μm sections of 10% formalin-fixed, paraffin-embedded skin. For the analysis shown in Figs 3*A–F* and 5, a signal amplification method based on the deposition of biotinylated tyramide was used as described previously (Kerstens *et al*, 1995). True blue peroxidase substrate (Kirkegaad & Perry Laboratories Inc., Gaithersburg, Maryland) was used as a color-developing reagent and nuclear fast red (Sigma, St Louis, Missouri) was used as a counterstain. For the analysis shown in Figs 3*G–K* and 4, the genes that have relatively abundant signals, and for objective comparison of the signal intensity among different hair cycle stages avoiding the bias by the manual handling *in situ* protocol, an automated slide-processing system (Discovery, Ventana Medical Systems, Inc., Tucson, Arizona) was used with protocols (Lindner *et al*, 1997), designed based on the standard protocol described in the RiboMap application note. Signals were detected automatically using the BlueMap NBT/BCIP substrate kit (Ventana, Tucson, Arizona) for 3 h at 37°C. For probe preparation, a mouse cDNA for each gene was amplified by RT-PCR using gene-specific primer sets listed in Table S2. Digoxigenin-labeled antisense and sense RNA probes were prepared by *in vitro* transcription with T7 RNA polymerase, using amplified cDNA of each gene as a template.

RT-PCR One microgram of total RNA was used for first-strand cDNA synthesis using superscript II (Invitrogen Corp., Carlsbad, California) according to the manufacturer's instructions; 1/50th of the synthesized cDNA was used as a template for PCR using Ampli-Taq Gold (PE Biosystems, Roppongi, Tokyo, Japan) and gene-specific primer sets listed in Table S2. After 10 min incubation at 94°C to activate the polymerase, each cDNA was amplified by the following iterative incubation 30 s at 94°C, 1 min at 55°C, and 1 min at 72°C with respective PCR cycles listed in Table S2 (shown as a supplement), separated on 1.5% agarose gels, and visualized by ethidium bromide staining.

Supplementary Material

The following supplementary material is available for this article online.
Figure S1 Overview of changes in gene expression during the hair cycle.
Table S1 Location of primers for RT-PCR and in-situ hybridization, and the number of PCR cycles for RT-PCR.
Table S2 Complete list of the genes up-regulated in late anagen and early catagen and fold-change during hair cycle.

DOI: 10.1111/j.0022-202X.2005.23825.x

Manuscript received September 9, 2004; revised March 8, 2005; accepted for publication March 21, 2005

Address correspondence to: Yumiko Ishimatsu-Tsuji, PhD, Shiseido Life Science Research Center, 2-12-1 Fukuura, Kanazawa-ku, Yokohama 236-8643 Japan. Email: yumiko.tsuji@to.shiseido.co.jp

References

Afonina E, Stauber R, Pavlakis GN: The human poly(A)-binding protein 1 shuttles between the nucleus and the cytoplasm. J Biol Chem 273:13015–13021, 1998

Anderson IC, Sugarbaker DJ, Ganju RK, *et al*: Stromelysin-3 is overexpressed by stromal elements in primary non-small cell lung cancers and regulated by retinoic acid in pulmonary fibroblasts. Cancer Res 55:4120–4126, 1995

Basset P, Bellocq JP, Wolf C, *et al*: A novel metalloproteinase gene specifically expressed in stromal cells of breast carcinomas. Nature 348:699–704, 1990

Boulay A, Masson R, Chenard MP, *et al*: High cancer cell death in syngeneic tumors developed in host mice deficient for the stromelysin-3 matrix metalloproteinase. Cancer Res 61:2189–2193, 2001

Carroll JM, McElwee KJ, E king L, Byrne MC, Sundberg JP: Gene array profiling and immunomodulation studies define a cell-mediated immune response underlying the pathogenesis of alopecia areata in a mouse model and humans. J Invest Dermatol 119:392–402, 2002

Daemen MA, Heemskerk VH, van't Veer C, Denecker G, Wolfs TG, Vandenabeele P, Buurman WA: Functional protection by acute phase proteins alpha(1)-acid glycoprotein and alpha(1)-antitrypsin against ischemia/reperfusion injury by preventing apoptosis and inflammation. Circulation 102:1420–1426, 2000

DasGupta R, Fuchs E: Multiple roles for activated LEF/TCF transcription complexes during hair follicle development and differentiation. Development 126:4557–4568, 1999

Delany AM, Canalis E: Dual regulation of stromelysin-3 by fibroblast growth factor-2 in murine osteoblasts. J Biol Chem 273:16595–16600, 1998

Deo RC, Bonanno JB, Sonenberg N, Burley SK: Recognition of polyadenylate RNA by the poly(A)-binding protein. Cell 98:835–845, 1999

Ferraris C, Chevalier G, Favier B, Jahoda CA, Dhouailly D: Adult corneal epithelium basal cells possess the capacity to activate epidermal, pilosebaceous and sweat gland genetic programs in response to embryonic dermal stimuli. Development 127:5487–5495, 2000

Gorlach M, Burd CG, Dreyfuss G: The mRNA poly(A)-binding protein: Localization, abundance, and RNA-binding specificity. Exp Cell Res 211:400–407, 1994

Goto T, Komai M, Bryant BP, Furukawa Y: Reduction in carbonic anhydrase activity in the tongue epithelium and submandibular gland in zinc-deficient rats. Int J Vitam Nutr Res 70:110–118, 2000

Hagglund AC, Basset P, Ny T: Stromelysin-3 is induced in mouse ovarian follicles undergoing hormonally controlled apoptosis, but this metalloproteinase is not required for follicular atresia. Biol Reprod 64:457–463, 2001

Hatse S, De Clercq E, Balzarini J: Role of antimetabolites of purine and pyrimidine nucleotide metabolism in tumor cell differentiation. Biochem Pharmacol 58:539–555, 1999

Hong HK, Noveroske JK, Headon DJ, Liu T, Sy MS, Justice MJ, Chakravarti A: The winged helix/forkhead transcription factor Foxq1 regulates differentiation of hair in satin mice. Genesis 29:163–171, 2001

Ikuzawa M, Yasumasu S, Inokuchi T, Kobayashi K, Nomura K, Iuchi I: Differential expression of two cathepsin Es during metamorphosis-associated remodeling of the larval to adult type epithelium in Xenopus stomach. J Biochem (Tokyo) 134:385–394, 2003

Ishizuya-Oka A, Li Q, Amano T, Damjanovski S, Ueda S, Shi YB: Requirement for matrix metalloproteinase stromelysin-3 in cell migration and apoptosis during tissue remodeling in *Xenopus laevis*. J Cell Biol 150:1177–1188, 2000

Karhumaa P, Leinonen J, Parkkila S, Kaunisto K, Tapanainen J, Rajaniemi H: The identification of secreted carbonic anhydrase VI as a constitutive glycoprotein of human and rat milk. Proc Natl Acad Sci USA 98:11604–11608, 2001

Kaufman CK, Zhou P, Pasolli HA, *et al*: GATA-3: An unexpected regulator of cell lineage determination in skin. Genes Dev 17:2108–2122, 2003

Kerstens HM, Poddighe PJ, Hanselaar AG: A novel *in situ* hybridization signal amplification method based on the deposition of biotinylated tyramine. J Histochem Cytochem 43:347–352, 1995

Kivela J, Parkkila S, Parkkila AK, Leinonen J, Rajaniemi H: Salivary carbonic anhydrase isoenzyme VI. J Physiol 520 (Part 2):315–320, 1999

Kligman AM: The human hair cycle. J Invest Dermatol 33:307–316, 1959

Kong J, Li XJ, Gavin D, Jiang Y, Li YC: Targeted expression of human vitamin D receptor in the skin promotes the initiation of the postnatal hair follicle cycle and rescues the alopecia in vitamin D receptor null mice. J Invest Dermatol 118:631–638, 2002

Levanon D, Goldstein RE, Bernstein Y, *et al*: Transcriptional repression by AML1 and LEF-1 is mediated by the TLE/Groucho corepressors. Proc Natl Acad Sci USA 95:11590–11595, 1998

Lin KK, Chudova D, Hatfield GW, Smyth P, Andersen B: Identification of hair cycle-associated genes from time-course gene expression profile data by using replicate variance. Proc Natl Acad Sci USA 101:5955–5960, 2004

Lindner G, Botchkarev VA, Botchkareva NV, Ling G, van der Veen C, Paus R: Analysis of apoptosis during hair follicle regression (catagen). Am J Pathol 151:1601–1617, 1997

Lutterbach B, Westendorf JJ, Linggi B, Isaac S, Seto E, Hiebert SW: A mechanism of repression by acute myeloid leukemia-1, the target of multiple chromosomal translocations in acute leukemia. J Biol Chem 275:651–656, 2000

Manes S, Mira E, Barbacid MM, *et al*: Identification of insulin-like growth factor-binding protein-1 as a potential physiological substrate for human stromelysin-3. J Biol Chem 272:25706–25712, 1997

Matziari M, Beau F, Cuniasse P, Dive V, Yiotakis A: Evaluation of P1'-diversified phosphinic peptides leads to the development of highly selective inhibitors of MMP-11. J Med Chem 47:325–336, 2004

Morris RJ, Liu Y, Marles L, *et al*: Capturing and profiling adult hair follicle stem cells. Nat Biotechnol 22:411–417, 2004

Muller-Rover S, Handjiski B, van der Veen C, *et al*: A comprehensive guide for the accurate classification of murine hair follicles in distinct hair cycle stages. J Invest Dermatol 117:3–15, 2001

Murphy G, Segain JP, O'Shea M, *et al*: The 28-kDa N-terminal domain of mouse stromelysin-3 has the general properties of a weak metalloproteinase. J Biol Chem 268:15435–15441, 1993

Nakanishi H, Tsukuba T, Kondou T, Tanaka T, Yamamoto K: Transient forebrain ischemia induces increased expression and specific localization of cathepsins E and D in rat hippocampus and neostriatum. Exp Neurol 121:215–223, 1993

Nishimura K, Ohki Y, Fukuchi-Shimogori T, *et al*: Inhibition of cell growth through inactivation of eukaryotic translation initiation factor 5A (eIF5A) by deoxyspergualin. Biochem J 363:761–768, 2002

Okada A, Tomasetto C, Lutz Y, Bellocq JP, Rio MC, Basset P: Expression of matrix metalloproteinases during rat skin wound healing: Evidence that membrane type-1 matrix metalloproteinase is a stromal activator of progelatinase A. J Cell Biol 137:67–77, 1997

Ostrander DB, O'Brien DJ, Gorman JA, Carman GM: Effect of CTP synthetase regulation by CTP on phospholipid synthesis in *Saccharomyces cerevisiae*. J Biol Chem 273:18992–19001, 1998

Park JH, Wolff EC, Folk JE, Park MH: Reversal of the deoxyhypusine synthesis reaction. Generation of spermidine or homospermidine from deoxyhypusine by deoxyhypusine synthase. J Biol Chem 278:32683–32691, 2003

Patil RV, Han Z, Yiming M, Yang J, Iserovich P, Wax MB, Fischbarg J: Fluid transport by human nonpigmented ciliary epithelial layers in culture: A homeostatic role for aquaporin-1. Am J Physiol Cell Physiol 281:C1139–C1145, 2001

Paus R, Handjiski B, Czarnetzki BM, Eichmuller S: Biology of the hair follicle. Hautarzt 45:808–25; quiz 824–825, 1994

Pei D, Majmudar G, Weiss SJ: Hydrolytic inactivation of a breast carcinoma cell-derived serpin by human stromelysin-3. J Biol Chem 269:25849–25855, 1994

Prasad AS: Zinc in growth and development and spectrum of human zinc deficiency. J Am Coll Nutr 7:377–384, 1988

Sachs AB, Bond MW, Kornberg RD: A single gene from yeast for both nuclear and cytoplasmic polyadenylate-binding proteins: Domain structure and expression. Cell 45:827–835, 1986

Seiberg M, Marthinuss J: Clusterin expression within skin correlates with hair growth. Dev Dyn 202:294–301, 1995

Seseke F, Thelen P, Ringert RH: Characterization of an animal model of spontaneous congenital unilateral obstructive uropathy by cDNA microarray analysis. Eur Urol 45:374–381, 2004

Singer CF, Marbaix E, Lemoine P, Courtoy PJ, Eeckhout Y: Local cytokines induce differential expression of matrix metalloproteinases but not their tissue inhibitors in human endometrial fibroblasts. Eur J Biochem 259:40–45, 1999

Soma T, Tsuji Y, Hibino T: Involvement of transforming growth factor-beta2 in catagen induction during the human hair cycle. J Invest Dermatol 118:993–997, 2002

Stenn KS, Paus R: Controls of hair follicle cycling. Physiol Rev 81:449–494, 2001

Thatcher BJ, Doherty AE, Orvisky E, Martin BM, Henkin RI: Gustin from human parotid saliva is carbonic anhydrase VI. Biochem Biophys Res Commun 250:635–641, 1998

Tumbar T, Guasch G, Greco V, Blanpain C, Lowry WE, Rendl M, Fuchs E: Defining the epithelial stem cell niche in skin. Science 303:359–363, 2004

Wada H, Hashimoto K, Wada Y, *et al*: Extensive oligonucleotide microarray transcriptome analysis of the rat cerebral artery and arachnoid tissue. J Atheroscler Thromb 9:224–232, 2002

Xu X, Lyle S, Liu Y, Solky B, Cotsarelis G: Differential expression of cyclin D1 in the human hair follicle. Am J Pathol 163:969–978, 2003

Yano K, Brown LF, Detmar M: Control of hair growth and follicle size by VEGF-mediated angiogenesis. J Clin Invest 107:409–417, 2001

Yano K, Brown LF, Lawler J, Miyakawa T, Detmar M: Thrombospondin-1 plays a critical role in the induction of hair follicle involution and vascular regression during the catagen phase. J Invest Dermatol 120:14–19, 2003

Zhou P, Byrne C, Jacobs J, Fuchs E: Lymphoid enhancer factor 1 directs hair follicle patterning and epithelial cell fate. Genes Dev 9:700–713, 1995

Journal of Dermatological Science (2005) 39, 147–154

ELSEVIER

Dermatological SCIENCE

www.intl.elsevierhealth.com/journals/jods

Hair cycle-specific expression of versican in human hair follicles

Tsutomu Soma*, **Masahiro Tajima, Jiro Kishimoto**

Shiseido Life Science Research Center, 2-12-1 Fukuura, Kanazawa-ku, Yokohama 236-8643, Japan

Received 25 November 2004; received in revised form 22 March 2005; accepted 28 March 2005

KEYWORDS
Androgenic alopecia;
Bulge;
Cytokeratin15;
Proteoglycans;
Stem cells

Summary

Background: Versican, a large chondroitin sulfate proteoglycan molecule, is implicated in the induction of hair morphogenesis, the initiation of hair regeneration, and the maintenance of hair growth in mouse species. In contrast, in human hair follicles, the distribution and the roles of versican remains obscure.
Objectives: To elucidate the implication of versican in normal human hair growth.
Methods: Versican expression was examined by in situ hybridization (mRNA) and immunohistochemistry (protein).
Results: The results clearly showed specific versican gene expression in the dermal papilla of anagen, which apparently decreased in the dermal papilla of catagen hair follicles. No specific signal was detectable in telogen hair follicles. Consistent with ISH results, versican immunoreactivity was extended over the dermal papilla of anagen hair follicles, and again, this staining diminished in the catagen phase of human hair follicles. Interestingly, versican proteins were deposited outside K15-positive epithelial cells in the bulge throughout the hair cycle. Versican immunoreactivity in the dermal papilla was almost lost in vellus-like hair follicles affected by male pattern baldness.
Conclusion: Specific expression of versican in the anagen hair follicles suggests its importance to maintain the normal growing phase of human as well as mouse.

1. Introduction

Mammalian hair follicles have a unique cyclical regrowth stage during their lifetime. Accordingly, evidence emphasizes the importance of epithelial–mesenchymal interaction for hair cycling between follicular stem cells and their specific mesenchymal dermal papilla (DP) cells. Compared with the recent progress of follicular stem cell research, the characterization of DP cells is virtually unknown, and one reason is the lack of a marker molecule, which shows relative specificity in its gene or protein expression for DP cells. One class of such candidate molecules is proteoglycans.

* Corresponding author. Tel.: +81 45 7887291; fax: +81 45 7887277.
E-mail address: tsutomu.souma@to.shiseido.co.jp (T. Soma).

0923-1811/$30.00
doi:10.1016/j.jdermsci.2005.03.010

Proteoglycans, a large family of glycosylated proteins, have covalently linked several sulfated glycosaminoglycans, such as chondroitin sulfate, dermatan sulfate, and heparan sulfate. The biological functions of proteoglycans involve development, cell adhesion, cell migration and differentiation to molecular signalling as well as a large number of water molecules [1,2]. Clinical patients with abnormal mucopolysaccharide metabolism (Hurler's syndrome) have very thick hair and a faster rate of hair growth during childhood [3]. Immunohistochemical studies with several proteoglycan-specific antibodies demonstrated the accumulation of glycosaminoglycan in the DP, particularly for chondroitin sulphate proteoglycan [4].

Versican is a chondroitin sulphate proteoglycan involved in matrix assembly and structure, and cell adhesion [5]. It is abundant in the dermis during human fetal skin development compared to adult skin. A recent transgenic study using a versican promoter implicated its expression in both mesenchymal condensation and hair induction during hair cycling [6]. Versican immunoreactivity is localized in the DP of active hair follicles (anagen) in mice and rats, but has not been elucidated in human species [7–9]. Here, we examined the onset of versican gene expression, and the deposition of versican protein durung human hair cycle to evaluate the implication of versican in normal human hair growth.

2. Materials and methods

2.1. Tissues, cells, and antibodies

Human tissue specimens from balding (three males, mean age 35 years) and non-balding (four males, two female, mean age 36 years) scalp-skin were obtained from plastic surgery with the informed consent of donors. DP cells were isolated from scalp tissues by micro-dissection, followed by in vitro cultivation. Mouse monoclonal anti-versican antibody (clone 2-B-1) purchased from Seikagaku Corp. (Tokyo, Japan) was applied at 10 μg/ml for both immunofluorescence and immunoperoxidase staining [10]. Chick polyclonal anti-cytokeratin 15 (K15) (provided by Covance Research Products Inc., Berkeley, CA) was used as a marker of the bulge region at 100-fold dilution.

2.2. RT-PCR

DP cells were cultured in Dubecco's modified minimal essential medium (Invitrogen, Carlsbad, CA) supplemented with 10% FBS. Total RNAs were extracted from the cultured DP cells with ISOGEN solution (Nippon Gene, Toyama, Japan), followed by the synthesis of first-strand cDNAs using oligo(dT) primers and Superscript II (Invitorgen, Carlsbad, CA). cDNA fragments of the human versican N-terminal-conserved domain (position 502–1160 in GenBank accession number X15998) were amplified by RT-PCR using total RNA from the human DP cells described above. Specific cDNA fragments of four versican variants (V0, V1, V2, and V3 isoforms) were amplified by RT-PCR using the primers listed in Table 1. All amplifications were performed for 35 cycles using the following conditions: 94 °C for 30 s, 58 °C for 30 s, and 72 °C for 1 min with High Fidelity PCR System (Roche Diagnostics, Indianapolis, IN). For the synthesis of anti-sense RNA probes, the recognition sequence of T7 polymerase was added to the anti-sense primers of each variant, which were applied by RT-PCR.

2.3. In situ hybridisation

For in situ hybridization (ISH), scalp tissue pieces were fixed in phosphate-buffered formalin (pH 7.2) for more than 1 week, then embedded in paraffin wax. Digoxigenin (DIG)-labeled anti-sense RNA probes were prepared with an in vitro transcription kit (Roche Diagnostics) using versican cDNA fragments containing the recognition sequence of T7 polymerase amplified by RT-PCR. DIG-labeled ISH was performed on 6 μm sections using the Ventana Discovery HX system (Ventana Japan, Yokohama, Japan) as described previously [11].

2.4. Immunofluorescence

For immunofluorescence staining, human scalp-skin pieces were fixed with 4% paraformaldehyde at 4 °C for 12–16 h, and then dehydrated and embedded in

Table 1 PCR primers for the amplification of versican isoforms

Primer	Sequence	Position[a]	Isoform	Primer pair	Size (bp)
F1	gctgcaaaagagtgtgaaaa	55408–55427	V0	F2 and R1	538
F2	tggtgaagaaacaaccagtg	65284–65303	V1	F1 and R1	501
F3	ctcatgttcctcccactacc	65331–65350	V2	F3 and R2	529
R1	agtggtaacgagatgcttcc	80518–80499	V3	F3 and R2	529
R2	tgggcaaagtatttgtagca	96685–96666			

[a] GenBank accession number AC026696.

paraffin wax. Tissue sections of 6 μm were boiled twice in 10 mM citrate-buffer (pH 6.0) for 5 min using a microwave oven for antigen relevance. Versican immunoreactivity was visualized with Alexa 594-labeled anti-mouse IgG antibody (Invitorgen). Chick anti-human keratin 15 (K15) polyclonal antibodies were used for double labeling with versican immunofluorescence visualized by FITC-labeled anti-mouse IgG antibody (Nakaraitecqure, Tokyo, Japan). K15 immunoreactivity was monitored with Alexa 594-labeled anti-chick IgG antibody (Invitorgen). All sections were mounted with a vector shield (Vector Labs, Burlingame, CA) containing 4′,6-diamidino-2-phenylindole (DAPI).

2.5. Immunoperoxidase staining

For immunoperoxidase staining, tissue sections were digested with proteinase K at 20 μg/ml for 30 min at room temperature (Nakaraitecque). The anti-mouse staining kit (HISTFINE, Nichirei, Tokyo, Japan) was used according to the manufacturer's instructions. Sections were developed with True Blue (Kirkegaard and Perry Labs, Gaithersburg, MD) followed by counterstaining with contrast red (Kirkegaard and Perry Labs).

3. Results

3.1. Predominant expression of versican transcripts in the DP of anagen hair follicles

Human cultured DP cells mainly expressed both V0 and V1 isoforms (Fig. 1) at RT-PCR level. To compare the expression level of versican isoforms in human hair follicles in vivo, we prepared 6 μm adjacent sections of human scalp-skin. Using ISH analysis on

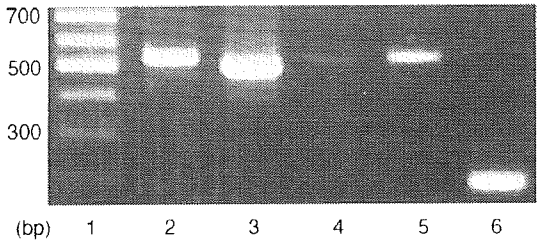

Fig. 1 RT-PCR analysis of versican isoforms in cultured DP cells. Total RNA of cultured DP cells was applied to RT-PCR analysis using isoform-specific primer pairs (Table). Lane 1, size marker (100 bp ladder); lane 2, V0; lane 3, V1; lane 4, V2; lane 5, V3; lane 6, GAPDH.

the adjacent sections, we revealed that human anagen hair follicles in vivo showed a predominant gene expression of V2 and V3 isoforms (Fig. 2C and D) in contrast to in vitro (see Fig. 1). The expression level of the V1 isoform (Fig. 2B) was equal to or lower than V2 and V3. Messenger RNAs of the V0 isoform (Fig. 2A) were not detectable, even in anagen hair follicles. cRNA probes for the N-terminal domain, shared among four isoforms, which should detect all versican isoforms, were applied to evaluate the versican gene expression during human hair cycles. The highest level of expression for versican mRNA was detected in the DP cells of human hair follicles in the anagen phase (Fig. 3A). Bulb matrix cells also expressed significant versican mRNA in anagen hair follicles (large arrows in Fig. 3A). Versican gene expression in the DP cells was dramatically reduced in the catagen phase, but was not completely lost (Fig. 3B). Cells in the upper portion of DP were still positive for versican mRNA expression (small arrows in Fig. 3B). Versican transcripts were not detectable in the DP of telogen hair follicles (Fig. 3C). We could not detect versican transcripts in either the epidermis or the dermis of adult scalp-skin tissues (data not shown).

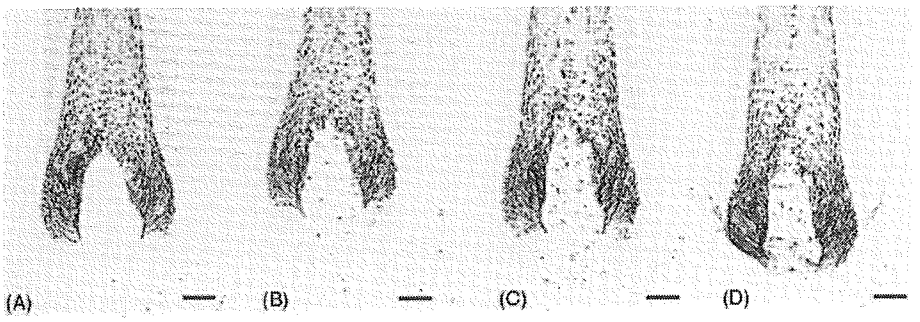

Fig. 2 In situ hybridization analysis of versican isoforms in the DP cells of anagen hair follicles. Adjacent sections were stained with the specific anti-sense RNA probe for each versican isoform. Blue staining indicated a positive signal for versican transcripts. (A) Endogenous mRNA expression of V0 isoform was not detected in the onion-shape DP at the bottom of anagen hair follicles. Melanin granules were observed as dark-brown colors in the hair shaft above the DP. (B) Expression level of V1 isoform was lower compared to V2 and V3 isoforms in the DP cells. (C) Signals of V2 isoform were almost equal to V3 isoform in the DP cells (D) [scale bars, 50 μm].